Interaction of a Screw Dislocation With an Arbitrary Shaped Elastic Inhomogeneity

Xu Wang

L. J. Sudak

Department of Mechanical and Manufacturing Engineering,
University of Calgary,
Calgary, Alberta,
Canada T2N-1N4

In this paper, the interaction between a screw dislocation and an arbitrary shaped elastic inhomogeneity with different material properties than the surrounding matrix is investigated. The exact solution to this problem is derived by means of complex variable methods and Faber series expansion. Specifically, the conformal mapping function maps the matrix region surrounding the inhomogeneity onto the outside of a unit circle in the image plane, while the analytic function defined in the elastic inhomogeneity is expressed in terms of a Faber series expansion. Once the series form solution is obtained, the stress fields due to the screw dislocation can be obtained. Also the image force on the screw dislocation due to its interaction with the elastic inhomogeneity is derived. Three examples of a screw dislocation interacting with (1) an equilateral triangular inhomogeneity, (2) a square inhomogeneity, and (3) a five-pointed star-shaped inhomogeneity are presented to illustrate how the stiffness of the triangular, square or five-pointed star-shaped inhomogeneity can influence the mobility of the screw dislocation.
[DOI: 10.1115/1.2073307]

1 Introduction

The interaction of dislocations with elastic inhomogeneities is an important topic in studying the strengthening and hardening mechanisms of materials. To simplify the analysis, most of the researchers assumed that the inhomoneneity is of circular shape (see, for example, [1,2]), is of elliptical shape (see [3–5] for details), or the inhomogeneity is rigid (or a cavity) with its shear modulus infinite (or zero) (see, for example, [6,7]).

Despite extensive study of inclusions with simple shapes, little effort has been devoted to inclusions of arbitrary shape. For example, Tsukrov and Novak [8] used a computational procedure to calculate the contribution of arbitrary shaped inclusions to the effective moduli of two-dimensional elastic solids. In [9,10], Ru developed a method for evaluating the stress fields of an arbitrary shaped inclusion embedded in full and half planes of isotropic and anisotropic elasticity, respectively. The key limitation of Ru's method is based on the assumption that elastic mismatch between dissimilar materials is negligible. Recently, the Faber series method [11] has been employed to study the problem of an arbitrary shaped inclusion perfectly bonded to the surrounding matrix. In particular, Gao and Noda [12] use the Faber series method to investigate the anti-plane problem of an arbitrary shaped piezoelectric inclusion embedded in an infinite piezoelectric medium.

The focus of the current paper is to investigate, in detail, the interaction problem of a screw dislocation with an arbitrary shaped elastic inhomogeneity. The main feature of this work is that the material properties of the inclusion and the surrounding matrix are different. The solution, in series form, is obtained by means of complex variable methods and Faber series expansion. A rigid inclusion or a cavity can be treated as a special case by letting the shear modulus of the inhomogeneity become infinite or zero, respectively. Once the solution is obtained, the stress fields in the inhomogeneity and in the matrix can be derived. In addition, the image force on the screw dislocation due to its interaction with the elastic inhomogeneity is also derived. In fact, we calculate the image force on the screw dislocation interacting with (1) an equilateral triangular inhomogeneity, (2) a square inhomogeneity, and (3) a five-pointed star-shaped inhomogeneity. It is found that the stiffness of the inhomogeneity has a significant influence on the nature of the image force (either attractive or repulsive) and also on the magnitude of the image force.

Contributed by the Applied Mechanics Division of ASME for publication in the JOURNAL OF APPLIED MECHANICS. Manuscript received January 27, 2005; final manuscript received May 17, 2005. Review conducted by Z. Sou. Discussion on the paper should be addressed to the Editor, Prof. Robert M. McMeeking, Journal of Applied Mechanics, Department of Mechanical and Environmental Engineering, University of California—Santa Barbara, Santa Barbara, CA 93106-5070, and will be accepted until four months after final publication in the paper itself in the ASME JOURNAL OF APPLIED MECHANICS.

2 Basic Formulations

As shown in Fig. 1, we consider a domain in R^2, infinite in extent, containing an arbitrary shaped elastic inhomogeneity with elastic properties different from those of the surrounding matrix. The linearly elastic materials occupying the inhomogeneity and matrix are assumed to be homogeneous and isotropic with shear moduli μ_1 and μ_2, respectively. We represent the matrix by the domain S_2 and assume that the inhomogeneity occupies the region S_1. The interface L separating the inhomogeneity and the surrounding matrix is assumed to be perfect (i.e., both the displacement and traction vectors are continuous across L). In addition, a screw dislocation with Burgers vector b is located at the point $z=z_0$ in the matrix.

For the anti-plane problem discussed in this paper, the displacement u_3, the stresses σ_{31}, σ_{32}, and resultant the force R_3 along any arc can be expressed in terms of a single analytic function $f(z)$ as

$$u_3 = \mathrm{Im}\{f(z)\},$$
$$\sigma_{32} + \mathrm{i}\sigma_{31} = \mu f'(z), \tag{1}$$
$$R_3 = -\mu \mathrm{Re}\{f(z)\}.$$

We consider the following conformal mapping function

$$z = m(\zeta) = R\left(\zeta + \sum_{n=1}^{+\infty} m_n \zeta^{-n}\right), \tag{2}$$

which maps the region occupied by the matrix to $|\zeta|>1$ in the mapped ζ plane.

Let the analytic functions in the inhomogeneity and the matrix be denoted by $f_1(z)$ and $f_2(z)$, respectively. For convenience, we write $f_i(z)=f_i(m(\zeta))=f_i(\zeta)$.

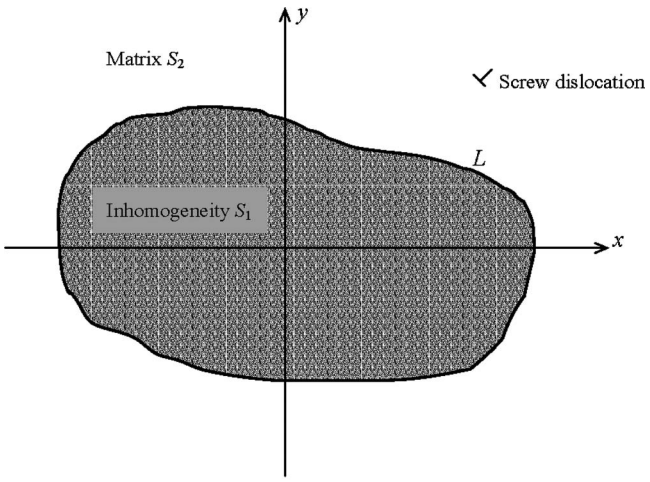

Fig. 1 A screw dislocation interaction with an arbitrarily shaped inhomogeneity

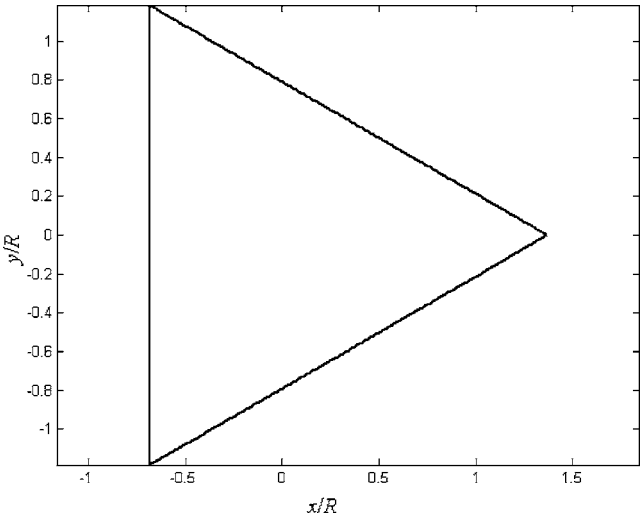

Fig. 2 The equilateral triangle described by Eq. (18)

3 Determination of $f_1(z)$ and $f_2(\zeta)$

The analytic function $f_1(z)$, defined within the inhomogeneity, can be expanded as a Faber series and expressed as follows:

$$f_1(z) = \sum_{n=1}^{+\infty} a_n P_n(z), \tag{3}$$

where $a_n (n=1,2,3,\cdots,+\infty)$ are unknown complex constants to be determined, and $P_k(z)$ is the kth degree Faber polynomial which can be explicitly expressed as

$$P_k(z) = P_k(m(\zeta)) = \zeta^k + \sum_{n=1}^{+\infty} \beta_{k,n}\zeta^{-n} (k = 1,2,3, \ldots, +\infty), \tag{4}$$

where the coefficients $\beta_{k,n}$ are determined by the following recurrence relations [12]

$$\begin{aligned} &\beta_{1,n} = m_n, \\ &\beta_{k+1,n} = m_{k+n} + \beta_{k,n+1} + \sum_{i=1}^{n} m_{n-i}\beta_{k,i}, \\ &\quad - \sum_{i=1}^{k} m_{k-i}\beta_{i,n} \quad (k,n = 1,2,3, \ldots, +\infty). \end{aligned} \tag{5}$$

Hence, $f_1(\zeta)$ can be expressed as follows:

$$f_1(\zeta) = \sum_{n=1}^{+\infty} \left[a_n\zeta^n + \left(\sum_{k=1}^{+\infty} a_k\beta_{k,n} \right) \zeta^{-n} \right]. \tag{6}$$

The continuity condition of displacement and traction across the interface $|\zeta|=1$ can be expressed as

$$\begin{aligned} &f_2^-(\zeta) - \bar{f}_2^+(1/\zeta) = f_1^+(\zeta) - \bar{f}_1^-(1/\zeta), \\ &f_2^-(\zeta) + \bar{f}_2^+(1/\zeta) = \Gamma[f_1^+(\zeta) + \bar{f}_1^-(1/\zeta)], (|\zeta| = 1), \end{aligned} \tag{7}$$

where $\Gamma = \mu_1/\mu_2$.

Inserting (6) into (7) yields the following:

$$\begin{aligned} f_2^-(\zeta) - \bar{f}_2^+(1/\zeta) = &\sum_{n=1}^{+\infty} \left[\left(a_n - \sum_{k=1}^{+\infty} \bar{a}_k\bar{\beta}_{k,n} \right) \zeta^n \right. \\ &\left. - \left(\bar{a}_n - \sum_{k=1}^{+\infty} a_k\beta_{k,n} \right) \zeta^{-n} \right], \\ f_2^-(\zeta) + \bar{f}_2^+(1/\zeta) = \Gamma &\sum_{n=1}^{+\infty} \left[\left(a_n + \sum_{k=1}^{+\infty} \bar{a}_k\bar{\beta}_{k,n} \right) \zeta^n \right. \\ &\left. + \left(\bar{a}_n + \sum_{k=1}^{+\infty} a_k\beta_{k,n} \right) \zeta^{-n} \right], \quad (|\zeta| = 1). \end{aligned} \tag{8}$$

Applying Liouville's theorem, we obtain two expressions for $f_2(\zeta)$

$$\begin{aligned} f_2(\zeta) = &- \sum_{n=1}^{+\infty} \left(\bar{a}_n - \sum_{k=1}^{+\infty} a_k\beta_{k,n} \right) \zeta^{-n} + \frac{b}{2\pi} \ln \frac{\zeta - 1/\bar{\zeta}_0}{\zeta} + \frac{b}{2\pi} \ln(\zeta - \zeta_0), \\ f_2(\zeta) = \Gamma &\sum_{n=1}^{+\infty} \left(\bar{a}_n + \sum_{k=1}^{+\infty} a_k\beta_{k,n} \right) \zeta^{-n} - \frac{b}{2\pi} \ln \frac{\zeta - 1/\bar{\zeta}_0}{\zeta} + \frac{b}{2\pi} \ln(\zeta \\ &- \zeta_0), \quad (|\zeta| > 1), \end{aligned} \tag{9}$$

where $\zeta = \zeta_0 = m^{-1}(z_0) (|\zeta_0| > 1)$ is the location of the screw dislocation.

In view of the fact that the two expressions for $f_2(\zeta)$ must be compatible with each other, then we arrive at the following set of algebraic equations:

$$(\Gamma + 1)a_n + (\Gamma - 1) \sum_{k=1}^{+\infty} \bar{\beta}_{k,n}\bar{a}_k = -\frac{b\zeta_0^{-n}}{n\pi} \quad (n = 1,2,3,\ldots,+\infty). \tag{10}$$

Truncating the above infinite system of linear algebraic equations at a sufficiently large integer N, we obtain

$$\mathbf{A}\mathbf{x} + \mathbf{B}\bar{\mathbf{x}} = \mathbf{f}, \tag{11}$$

where

$$\mathbf{A} = (\Gamma + 1)\mathrm{diag}[1 \quad 1 \quad \cdots \quad 1], \tag{12a}$$

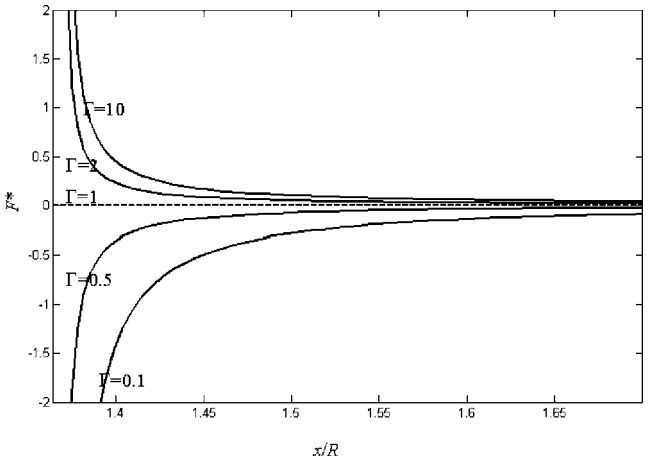

Fig. 3 The normalized image force on a screw dislocation located on the positive *x* axis interacting with the equilateral triangular inhomogeneity

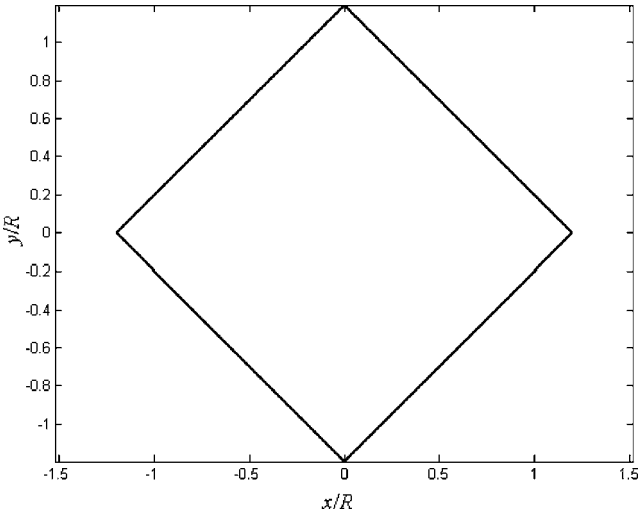

Fig. 4 The square described by Eq. (20)

$$\mathbf{B} = (\Gamma - 1)\begin{bmatrix} \bar{\beta}_{1,1} & \bar{\beta}_{2,1} & \cdots & \bar{\beta}_{N,1} \\ \bar{\beta}_{1,2} & \bar{\beta}_{2,2} & \cdots & \bar{\beta}_{N,2} \\ \vdots & \vdots & \ddots & \vdots \\ \bar{\beta}_{1,N} & \bar{\beta}_{2,N} & \cdots & \bar{\beta}_{N,N} \end{bmatrix},$$

$$\mathbf{x} = \begin{bmatrix} a_1 \\ a_2 \\ \vdots \\ a_N \end{bmatrix}, \quad \mathbf{f} = -\frac{b}{\pi}\begin{bmatrix} \dfrac{1}{\zeta_0} \\ \dfrac{1}{2\zeta_0^2} \\ \vdots \\ \dfrac{1}{N\zeta_0^N} \end{bmatrix}. \tag{12b}$$

The above set of algebraic equations can be resolved to give

$$\begin{bmatrix} \mathbf{x} \\ \bar{\mathbf{x}} \end{bmatrix} = \begin{bmatrix} \mathbf{A} & \mathbf{B} \\ \bar{\mathbf{B}} & \mathbf{A} \end{bmatrix}^{-1}\begin{bmatrix} \mathbf{f} \\ \bar{\mathbf{f}} \end{bmatrix}. \tag{13}$$

Remark: The two analytic functions $f_1(z)$ and $f_2(\zeta)$ have now been uniquely determined.

4 Stress Field

Once the analytic function $f_1(z)$ for the inhomogeneity is obtained, the stress field within the arbitrary shaped inhomogeneity can be expressed as

$$\sigma_{32} + \mathrm{i}\sigma_{31} = \mu_1 \sum_{n=1}^{+\infty} a_n P_n'(z). \tag{14}$$

Particularly, the stresses within the inhomogeneity are distributed along the interface L as follows:

$$\sigma_{32} + \mathrm{i}\sigma_{31} = \mu_1 \frac{\displaystyle\sum_{n=1}^{+\infty} n\left[a_n\zeta^{n-1} - \left(\sum_{k=1}^{+\infty} a_k\beta_{k,n}\right)\zeta^{-n-1}\right]}{R\left(1 - \displaystyle\sum_{n=1}^{+\infty} m_n n\zeta^{-n-1}\right)} \quad (|\zeta| = 1). \tag{15}$$

Similarly, once the analytic function $f_2(\zeta)$ for the matrix is obtained, the stresses in the matrix are calculated to be

$$\sigma_{32} + \mathrm{i}\sigma_{31} = \mu_2 \frac{\displaystyle\sum_{n=1}^{+\infty} n\left(\bar{a}_n - \sum_{k=1}^{+\infty} a_k\beta_{k,n}\right)\zeta^{-n-1} + (b/2\pi)([1/\zeta(\bar{\zeta}_0\zeta - 1)] + [1/(\zeta - \zeta_0)])}{R\left(1 - \displaystyle\sum_{n=1}^{+\infty} m_n n\zeta^{-n-1}\right)}, (|\zeta| > 1). \tag{16}$$

5 Image Force on the Screw Dislocation

The image force acting on the screw dislocation due to its interaction with the arbitrary shaped elastic inhomogeneity is derived and takes the following form:

$$F_x - \mathrm{i}F_y = \frac{\mu_2 b\left[\displaystyle\sum_{n=1}^{+\infty} n\left(\bar{a}_n - \sum_{k=1}^{+\infty} a_k\beta_{k,n}\right)\zeta_0^{-n-1} - \{(b/4\pi)[\sum_{n=1}^{+\infty} m_n n(n+1)\zeta_0^{-n-2}/(1 - \sum_{n=1}^{+\infty} m_n n\zeta_0^{-n-1})]\} + \{(b/2\pi)[1/\zeta_0(|\zeta_0|^2 - 1)]\}\right]}{R\left(1 - \displaystyle\sum_{n=1}^{+\infty} m_n n\zeta_0^{-n-1}\right)} (|\zeta_0| > 1), \tag{17}$$

where F_x and F_y are respectively the x and y components of the material force.

6 Examples

6.1 An Equilateral Triangular Inhomogeneity. First, let us consider a screw dislocation interacting with an equilateral triangular inhomogeneity. The specific conformal mapping function is taken to be the following (see, for example, [13,14]):

$$z = m(\zeta) = R\left(\zeta + \frac{1}{3}\zeta^{-2} + \frac{1}{45}\zeta^{-5} + \cdots + \frac{(-1)^k}{(1-3k)}C_{2/3}{}^k\zeta^{1-3k} + \cdots\right) \quad (R>0). \tag{18}$$

In this paper, the above mapping function is truncated at $k=50$ and we take $N=150$ to ensure that the obtained results are sufficiently accurate. The equilateral triangle described by the above mapping function is illustrated in Fig. 2. The calculated coefficients $\beta_{k,n}$ $(k,n=1,2,3,\ldots,10)$ are given by

$$[\beta] = \begin{bmatrix} 0 & 0.3333 & 0 & 0 & 0.0222 & 0 & 0 & 0.0062 & 0 & 0 \\ 0.6667 & 0 & 0 & 0.1556 & 0 & 0 & 0.0272 & 0 & 0 & 0.0098 \\ 0 & 0 & 0.4000 & 0 & 0 & 0.1000 & 0 & 0 & 0.0291 & 0 \\ 0 & 0.3111 & 0 & 0 & 0.2321 & 0 & 0 & 0.0719 & 0 & 0 \\ 0.1111 & 0 & 0 & 0.2901 & 0 & 0 & 0.1497 & 0 & 0 & 0.0567 \\ 0 & 0 & 0.2000 & 0 & 0 & 0.2182 & 0 & 0 & 0.1055 & 0 \\ 0 & 0.0951 & 0 & 0 & 0.2096 & 0 & 0 & 0.1599 & 0 & 0 \\ 0.0494 & 0 & 0 & 0.1437 & 0 & 0 & 0.1827 & 0 & 0 & 0.1199 \\ 0 & 0 & 0.0873 & 0 & 0 & 0.1582 & 0 & 0 & 0.1493 & 0 \\ 0 & 0.0492 & 0 & 0 & 0.1135 & 0 & 0 & 0.1499 & 0 & 0 \end{bmatrix}. \tag{19}$$

Figure 3 demonstrates the normalized image force, $F^* = RF_x/\mu_2 b^2$, on the screw dislocation which is located on the positive x axis in the matrix. It is observed that the screw dislocation will be attracted to the triangular inhomogeneity (i.e. $F_x<0$) when the inhomogeneity is softer than the surrounding matrix ($\Gamma<1$) and the magnitude of the attractive force will be higher when Γ ($\Gamma<1$) becomes smaller and the dislocation is closer to the tip of the inhomogeneity. On the other hand, the triangular inhomogeneity will repel the screw dislocation (i.e. $F_x>0$) when the inhomogeneity is stiffer than the surrounding matrix ($\Gamma>1$) and the magnitude of the repulsive force will be higher when $\Gamma(\Gamma>1)$ becomes larger and the dislocation is closer to the tip of the inhomogeneity.

6.2 A Square Inhomogeneity. Next, we address a screw dislocation interacting with a square inhomogeneity. The specific conformal mapping function is taken to be the following (see, for example, [13,14])

$$z = m(\zeta) = R\left[\zeta + \frac{1}{6}\zeta^{-3} + \frac{1}{57}\zeta^{-7} + \cdots + \frac{(-1)^k}{(1-4k)}C_{1/2}{}^k\zeta^{1-4k} + \cdots\right] \quad (R>0). \tag{20}$$

The above mapping function is truncated at $k=50$ and we take $N=200$. The square described by the above mapping function is illustrated in Fig. 4. The calculated coefficients $\beta_{k,n}$ $(k,n=1,2,3,\ldots,10)$ are given by

$$[\beta] = \begin{bmatrix} 0 & 0 & 0.1667 & 0 & 0 & 0 & 0.0179 & 0 & 0 & 0 \\ 0 & 0.3333 & 0 & 0 & 0 & 0.0635 & 0 & 0 & 0 & 0.0173 \\ 0.5000 & 0 & 0 & 0 & 0.1369 & 0 & 0 & 0 & 0.0395 & 0 \\ 0 & 0 & 0 & 0.2381 & 0 & 0 & 0 & 0.0770 & 0 & 0 \\ 0 & 0 & 0.2282 & 0 & 0 & 0 & 0.1193 & 0 & 0 & 0 \\ 0 & 0.1905 & 0 & 0 & 0 & 0.1525 & 0 & 0 & 0 & 0.0728 \\ 0.1250 & 0 & 0 & 0 & 0.1671 & 0 & 0 & 0 & 0.0977 & 0 \\ 0 & 0 & 0 & 0.1539 & 0 & 0 & 0 & 0.1175 & 0 & 0 \\ 0 & 0 & 0.1186 & 0 & 0 & 0 & 0.1256 & 0 & 0 & 0 \\ 0 & 0.0866 & 0 & 0 & 0 & 0.1214 & 0 & 0 & 0 & 0.0943 \end{bmatrix}. \tag{21}$$

Figure 5 demonstrates the normalized image force, $F^* = RF_x/\mu_2 b^2$, on the screw dislocation located on the positive x axis in the matrix. The phenomenon observed for the square inhomogeneity is identical to that for an equilateral triangular inhomogeneity.

6.3 A Five-Pointed Star-Shaped Inhomogeneity. Finally, we investigate a screw dislocation interacting with a five-pointed star-shaped inhomogeneity. The specific conformal mapping function is taken to be the following [13]:

$$z = m(\zeta) = R\left[\zeta + \sum_{p=1}^{+\infty}\left(\sum_{k=0}^{p}(-1)^k C_{4/5}{}^k C_{-2/5}{}^{p-k}\right)\frac{1}{1-5p}\zeta^{1-5p}\right] \quad (R>0). \tag{22}$$

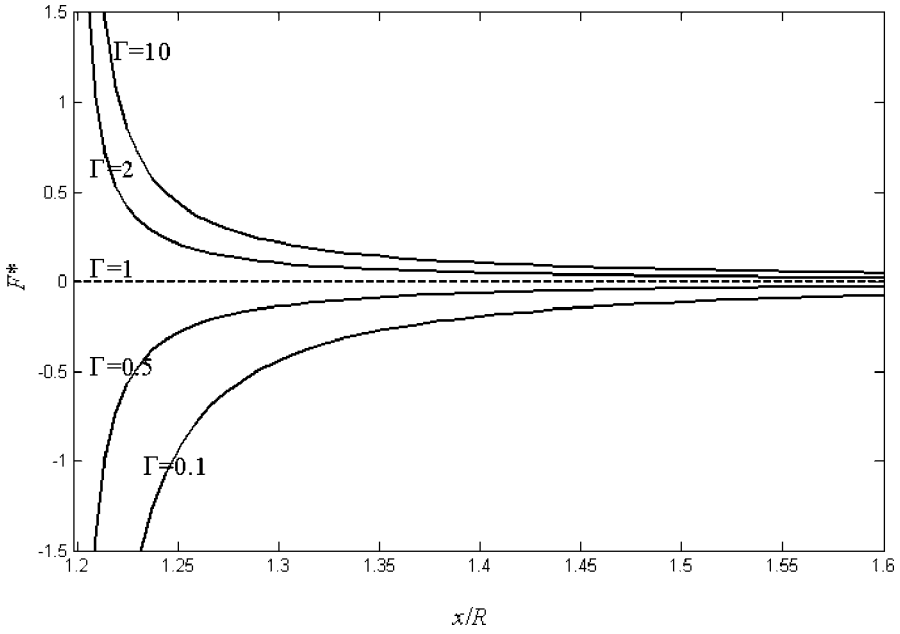

Fig. 5 The normalized image force on a screw dislocation located on the positive *x* axis interacting with the square inhomogeneity

Notice that there is a misprint in Eq. (27) of Ref. [13]. "$2/n$" should read "$-2/n$." The above mapping function is truncated at $p=500$ and we take $N=250$. The five-pointed star described by the mapping function Eq. (22) is illustrated in Fig. 6. The calculated coefficients $\beta_{k,n}$ $(k,n=1,2,3,\ldots,10)$ are given by

$$[\beta]=\begin{bmatrix} 0 & 0 & 0 & 0.3 & 0 & 0 & 0 & 0 & -0.0578 & 0 \\ 0 & 0 & 0.6 & 0 & 0 & 0 & 0 & -0.0256 & 0 & 0 \\ 0 & 0.9 & 0 & 0 & 0 & 0 & 0.0967 & 0 & 0 & 0 \\ 1.2 & 0 & 0 & 0 & 0 & 0.3089 & 0 & 0 & 0 & 0 \\ 0 & 0 & 0 & 0 & 0.6111 & 0 & 0 & 0 & 0 & 0.0833 \\ 0 & 0 & 0 & 0.4633 & 0 & 0 & 0 & 0 & 0.3160 & 0 \\ 0 & 0 & 0.2256 & 0 & 0 & 0 & 0 & 0.4947 & 0 & 0 \\ 0 & -0.1022 & 0 & 0 & 0 & 0 & 0.5653 & 0 & 0 & 0 \\ -0.52 & 0 & 0 & 0 & 0 & 0.4740 & 0 & 0 & 0 & 0 \\ 0 & 0 & 0 & 0 & 0.1667 & 0 & 0 & 0 & 0 & 0.4130 \end{bmatrix}. \tag{23}$$

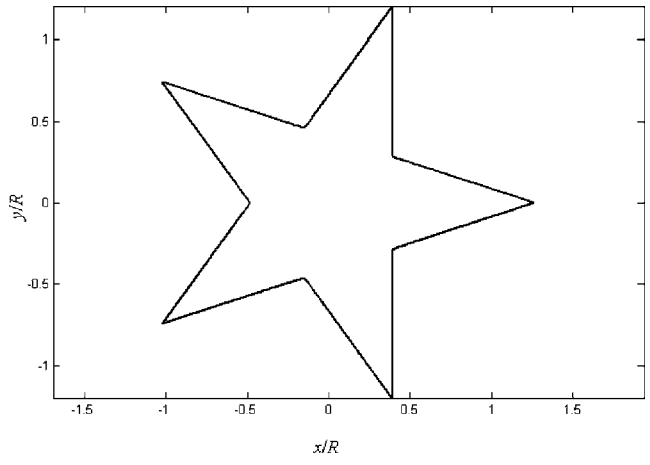

Fig. 6 The five-pointed star described by Eq. (22)

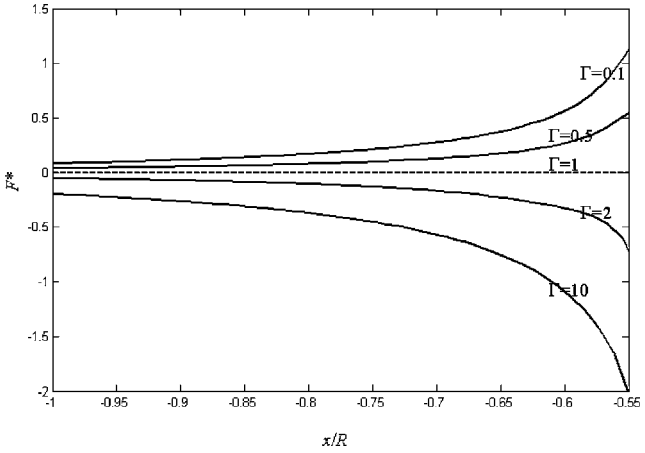

Fig. 7 The normalized image force on a screw dislocation located on the *negative x* axis interacting with the five-pointed star-shaped inhomogeneity

Figure 7 demonstrates the normalized image force, $F^* = RF_x/\mu_2 b^2$, on the screw dislocation located on the *negative x* axis in the matrix. By noting that the dislocation will be attracted to the inhomogeneity when $F_x > 0$, and the dislocation will be repelled from the inhomogeneity when $F_x < 0$, then the phenomenon observed here is similar to that observed for an equilateral triangular or a square inhomogeneity, respectively.

7 Conclusions

In this paper, we present the problem of a screw dislocation interacting with an arbitrary shaped elastic inhomogeneity. The key feature of this work is that the material properties of the inhomogeneity and the surrounding matrix are different. Through the introduction of a conformal mapping function, the region occupied by the matrix can be mapped to the outside of a unit circle in the ζ-plane. In addition, the analytic function defined in the elastic inhomogeneity is expanded into a Faber series. Once the series form solution is obtained, the stress fields due to the screw dislocation can be obtained. Also the image force on the screw dislocation due to its interaction with the elastic inhomogeneity is derived. Several examples of practical importance are presented to demonstrate the feasibility of the obtained solution and to illustrate the influence of the stiffness of the elastic inhomogeneity on the mobility of the screw dislocation. The case where the screw dislocation lies in the arbitrary shaped elastic inhomogeneity can also be similarly addressed. As well, the obtained solution can be easily applied to investigate a matrix crack interacting with an arbitrary shaped elastic inhomogeneity.

Acknowledgment

This work is supported by the Natural Sciences and Engineering Research Council of Canada through grand NSERC No. 249516.

References

[1] Dundurs, J., and Mura, T., 1964, "Interaction Between an Edge Dislocation and a Circular Inclusion," J. Mech. Phys. Solids **12**, pp. 177–189.
[2] Dundurs, J., 1967, "On the Interaction of a Screw Dislocation With Inhomogeneities," Recent Adv. Eng. Sci., **2**, pp. 223–233.
[3] Sendeckyj, G. P., 1970, "Fundamental Aspects of Dislocation Theory". J. A. Summons, Wit R. De, and R. Bulouch, eds., National Bureau of Standards (U.S.), Special Publication 317, Vol. I, p. 57.
[4] Stagni, L., and Lizzio, R., 1983, "Shape Effects in the Interaction Between an Edge Dislocation and an Elliptical Inhomogeneity," Appl. Phys. A: Solids Surf. **A30**, pp. 217–221.
[5] Chen, D. H., 1994, "Interference Between an Elliptical Inclusion and Point Force or Dislocation," J. Jpn. Soci. Mech. Engi., **60**, pp. 2796–2801.
[6] Wu, K. C., 1992, "Interaction of a Dislocation With an Elliptic Hole or Rigid Inclusion in an Anisotropic Material," J. Appl. Phys. **72**, pp. 2156–2163.
[7] Santare, M. H., and Keer, L. M., 1986, "Interaction Between an Edge Dislocation and a Rigid Elliptic Inclusion," ASME J. Appl. Mech. **53**, pp. 382–385.
[8] Tsukrov, I., and Novak, J., 2004, "Effective Elastic Properties of Solids With Two-dimensional Inclusions of Irregular Shapes," Int. J. Solids Struct. **41**, pp. 6905–6924.
[9] Ru, C. Q., 1999, "Analytic Solution for Eshelby's Problem of an Inclusion of Arbitrary Shape in a Plane or Half-plane," ASME J. Appl. Mech. **66**, pp. 315–322.
[10] Ru, C. Q., 2003, "Eshelby Inclusion of Arbitrary Shape in an Anisotropic Plane or Half-plane," Acta Mech. **160**, pp. 219–234.
[11] Curtiss, J. H., 1971, "Faber Polynomials and Faber Series," Am. Math. Monthly **78**, pp. 577–596.
[12] Gao, C. F., and Noda, N., 2004, "Faber Series Method for Two-dimensional Problems of Arbitrarily Shaped Inclusion in Piezoelectric Materials," Acta Mech. **171**, pp. 1–13.
[13] Chen, T., and Chiang, S. C., 1997, "Electroelastic Fields and Effective Moduli of a Medium Containing Cavities or Rigid Inclusions of Arbitrary Shape Under Anti-plane Mechanical and In-plane Electric Fields," Acta Mech. **121**, pp. 79–96.
[14] Thorpe, M. F., 1992, "The Conductivity of a Sheet Containing a few Polygonal Holes or Superconducting Inclusions," Proc. R. Soc. London, Ser. A **437**, pp. 215–227.